Plasmon Reflection Reveals Local Electronic Properties of Natural Graphene Wrinkles

To cite this article before publication: Runkun Chen *et al* 2019 *Chinese Phys. B* in press https://doi.org/10.1088/1674-1056/ab46a2

Plasmon Reflection Reveals Local Electronic Properties of Natural Graphene Wrinkles

Runkun Chen(陈闰堃)[1], Cui Yang(杨翠)[1], Yuping Jia(贾玉萍)[2,3], Liwei Guo(郭丽伟)[4,5,6,†], and Jianing Chen(陈佳宁)[1,6,†]

[1]*Beijing National Laboratory for Optical Physics, Institute of Physics, Chinese Academy of Sciences, University of Chinese Academy of Sciences, Beijing 100190, P. R. China*

[2]*Beijing National Laboratory for Condensed Matter Physics, Institute of Physics, Chinese Academy of Sciences, Beijing 100190, P. R. China*

[3]*Changchun Institute of Optics, Fine Mechanics and Physics, Chinese Academy of Sciences Jilin 130033, P. R. China*

[4]*Research and Development Center for Functional Crystals, Laboratory of Advanced Materials and Electron Microscopy, Beijing National Laboratory for Condensed Matter Physics, Institute of Physics, Chinese Academy of Sciences, Beijing 100190, P. R. China*

[5]*Center of Materials Science and Optoelectronics Engineering, University of Chinese Academy of Sciences, Beijing 100190, P. R. China*

[6]*Songshan Lake Materials Laboratory Dongguan, 523808 Guangdong, China*

We systematically studied surface plasmons reflection by graphene wrinkles with different heights on SiC substrate. Combined with numerical simulation, we found the geometry corrugation of a few nanometer height of wrinkle alone does not causes a reflection of graphene plasmons. Instead, the separated wrinkle from substrate exhibits a nonlinear spatial Fermi energy distribution along the wrinkle, which acts as a heterojunction. Therefor a higher graphene wrinkle induces stronger damped region when propagating graphene surface plasmons encounter the wrinkle and get reflected.

Keywords: graphene plasmons, wrinkle, reflection, electronic

PACS: 73.20.Mf, 61.48.Gh, 72.80.Vp

[*] This work was supported by the National Key Research and Development Program of China (2016YFA0203500), National Natural Science Foundation of China (Grant No.11874407), and Strategic Priority Research Program of Chinese Academy of Science (Grant No. XDB 30000000).

[†] Corresponding author. E-mail: lwguo@iphy.ac.cn

[†] Corresponding author. E-mail: jnchen@iphy.ac.cn

1. Introduction

Surface plasmons polariton, coupling between collective oscillation of free carriers and the excitation light, was strongly confined at the metal-medium interface, which has great potential in the plasmonics devices.[1-8] Moreover, graphene has tunable carrier concentration and high carrier mobility [9-13] which supporting plasmons propagation on a 2-dimensional plane in infrared regimes and draws great of interests in electronics and plasmonics.[14-16] Epitaxial graphene grown on SiC substrate is widely used to obtain large area and high crystal quality graphene,[17, 18] and has a great potential to electronics applications[19] and graphene-based plasmonics devices.[20-23] However, due to the compressive strain caused by the different thermal expansion coefficient of graphene and SiC on the annealing process, graphene wrinkle is widely existed on the epitaxial graphene.[24-26] The most important issue for graphene based devices is the electronic property of wrinkle and how these wrinkles affect the graphene plasmons.

Based on the near-field optical technology, researchers observed graphene plasmons reflected by edges,[14] steps,[21] or grain boundaries[27] in the real-space by scattering scanning near-field microscopy. It is also proved[27] that the grain boundaries form electronic barriers and affect electronic transport properties. Graphene plasmons reflection by different conductivity patterns in a flat graphene[28] and by a geometry corrugation structure[29] have been study theoretically. However, experimental study of graphene plasmons reflected by a nanometer sized graphene structure such as wrinkle has not been reported. Herein, we characterize the graphene wrinkle with Raman spectroscopy, and then utilize the scattering scanning near field optical microscopy (s-SNOM) to study how wrinkle affects the graphene plasmons propagation. Focusing on the near-field infrared imaging of graphene plasmons propagating along epitaxial graphene on a SiC substrate, we observe a novel interferences pattern between the tip-emitted and back-reflected graphene plasmons at the natural wrinkle. Combined with the numerical simulation, we conclude that the wrinkle separated with substrate forming a heterojunction with neighbor graphene due to obvious difference in carrier concentration, which induces a strong reflection of graphene plasmons compared to the negligible reflection of the geometry corrugation. These results suggest that the graphene wrinkle has nonlinear localized electronic property with important impact on graphene integrated electronic devices. We show that it is possible to conduct optical, touching free method to explore local electronic properties of fine structures in graphene as well as in principle other 2D materials.

2. Results and Discussion

To investigate the graphene surface plasmons on the epitaxial monolayer graphene, an infrared near field imaging experiment is conducted by s-SNOM. The schematics of experiment is shown in **Figure 1(a)**. The atomic force microscopy (AFM) probe, with radius about 25 nm, can compensate the momentum mismatch between the incident light and the surface plasmons then excite the surface plasmons.[14, 15, 21] In order to suppress background signal of the scattering signal from the tip and samples, pseudo-heterodyne interferometric detection scheme is used to demodulate the detected signal at a higher harmonic n (n=3 in this paper), then subtracts the background from the collected signal.[30] Finally, we obtain the topography structure and graphene plasmons imaging simultaneously when the tip scanning across the epitaxial graphene sample.

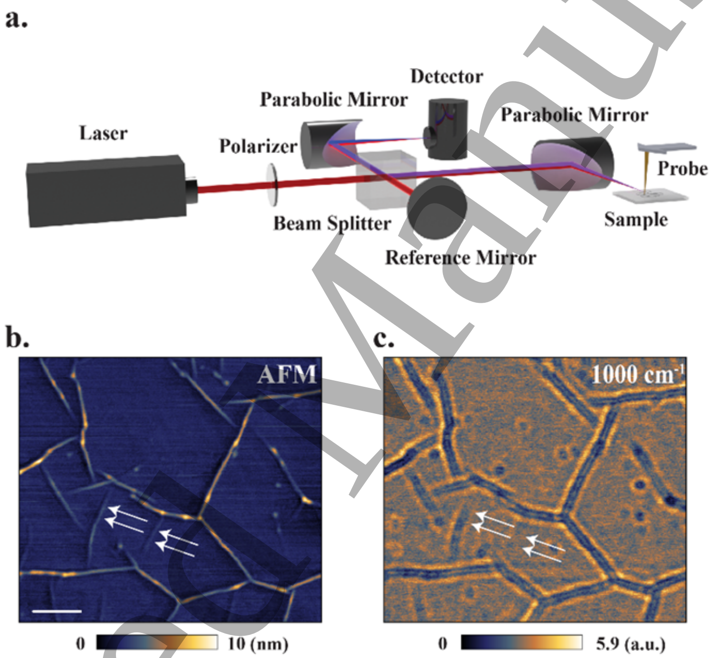

Figure 1. Near field infrared imaging of graphene plasmons on SiC substrate. (a) The schematic diagram of s-SNOM experiment. (b) AFM topography image of graphene wrinkles on SiC substrate. (c) The corresponding infrared near field amplitude image of (b) at the frequency of 1000 cm^{-1}. The scale bar is 500 nm.

Figure 1(b) is the precise AFM topography image of epitaxial graphene. To characterize the quality of the epitaxial graphene and the raised mesh structure in **Figure 1(b)**, a Raman measurement is carried. The Raman spectroscopy of epitaxial graphene sample on SiC substrate is shown in **Figure 2**. In **Figure 2(a)**, the Raman spectra of the bare SiC substrate (black solid line) and epitaxial graphene on SiC (blue solid line) are plotted respectively. The Raman spectra of the pure graphene is plotted in **Figure 2(b)** by subtracting the background spectra of SiC substrate. It seems that the epitaxial graphene is more than one layer due to the intensity of 2D peak is stronger than the intensity of SiC peak (1519 cm^{-1}). We attribute it to the focus of laser spot is above the graphene surface, which can also be found in the previous research.[31] The ratio of I_{2D}/I_G is about 5 and the full-width half-maximum (FWHM) of 2D band is 23.25 cm^{-1} (inset of **Fig.2b**), which indicate that graphene grown on the SiC substrate is a monolayer graphene.[32-34] Furthermore, the absence of D band (~1350 cm^{-1}) means a high quality of crystal structure in the monolayer epitaxial graphene,[32, 35] which suggests the raised structure in **Figure 2(b)** is a continuous graphene wrinkle and no edge or crack exist. (More information of the Raman mappings of the epitaxial monolayer graphene are shown in **Figure S1** in Supporting Information). **Figure 1(c)** is the optical near-field amplitude image (3th harmonics) at an incident frequency of 1000 cm^{-1} corresponding to the same region in **Figure 1(b)**. An obvious feature is observed that a brightest twin fringes occur outside and parallel to the wrinkle. It is similar with the previous reported[27] where graphene plasmons reflect by the grain boundaries. In **Figure 3**, we analyze a 1*1 um^2 zoom in area in **Figure 1(b)**, which has a higher resolution. The topography and near field infrared imaging are shown in **Figure 3(a)** and **(b)**, respectively. The topography height and normalized near field amplitude of line profiles taken along the white dash lines in **Figure 3(a)** and **(b)** are shown in **Figure 3(c)**. It is clear that the bright fringe occurs outside the wrinkle. Furthermore, the width of fringe FW also changes with the incident light. Here we compare the theoretical graphene plasmons wavelength on SiC substrate and the fringe width in **Figure 3(d)**. The black square is two times of fringe width extracted from experiments and the blue curve represents the theoretical relation of graphene plasmons on SiC substrate. It is noteworthy that the fringe width is in good agreement with theoretical dispersion of graphene plasmons, which certifies that the fringe is the interference of the tip-emitted and back-reflected plasmons by the wrinkle.[14, 15, 27]

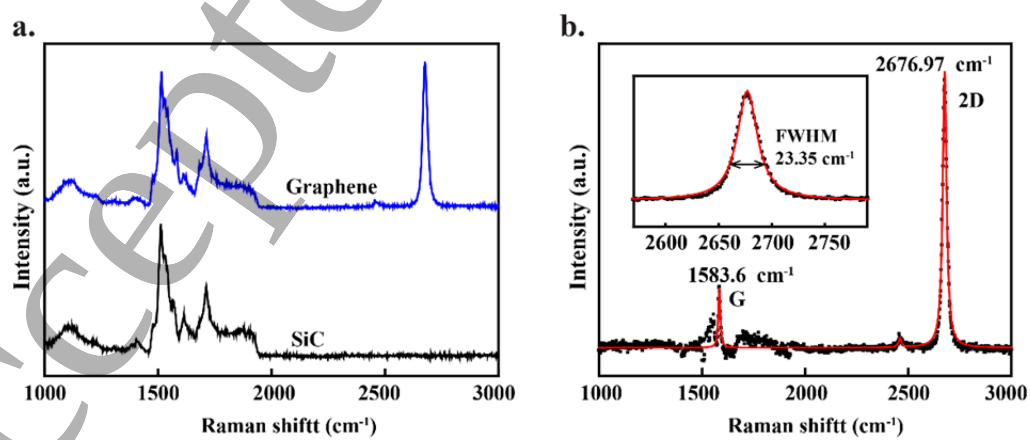

Figure 2. The Raman spectroscopy of epitaxial monolayer graphene on SiC substrate. (a) Raman spectra of graphene and SiC substrate, respectively. (b) Raman spectra of monolayer graphene on SiC after subtracting the SiC background. The inset is Lorentz fitting of 2D band.

There is also an important feature that the amplitude of fringes is related with the height of graphene wrinkles in **Figure 1(b)** and **(c)**. As shown in **Figure 1(b)**, most of wrinkles height on the epitaxial graphene are about 3 nm, and only a few wrinkles are lower than 1 nm. The higher wrinkles show an obviously interference fringes in **Figure 1(c)**. However, the wrinkles with lower height as indicated by the white arrows in **Figure 1(b)** exhibit a very weak or no fringes as shown in **Figure 1(c)**. (We extract the fringes amplitude profiles around different height of wrinkle in Supporting Information). It appears that the graphene plasmons reflection increases with the heights of wrinkle. In order to figure out how graphene plasmons reflected by wrinkle, we conduct a numerical simulation with the finite element method. The schematic of simulation model in our simulation is shown in **Figure 4(a)**. In the simulation model, the scanning metallic tip is treated as a point dipole with a vertically oriented momentum and the graphene with wrinkle is modelled as a surface current with $\boldsymbol{J} = \sigma\boldsymbol{E}$. Then the intensity of electric field |E|, is recorded by a point probe under the electric dipole when the electric dipole scanning across the graphene. Shown as the grey line in **Figure 4(b)**, we calculate the electric field profile when the dipole scanning across the graphene wrinkle. Compared with the experiment data (black dot line), it suggests that the reflection by the topographic shape of wrinkle is negligible and the strong reflection in the experiment should be caused by other reason. (More simulation with different heights of wrinkle are in Supporting Information)

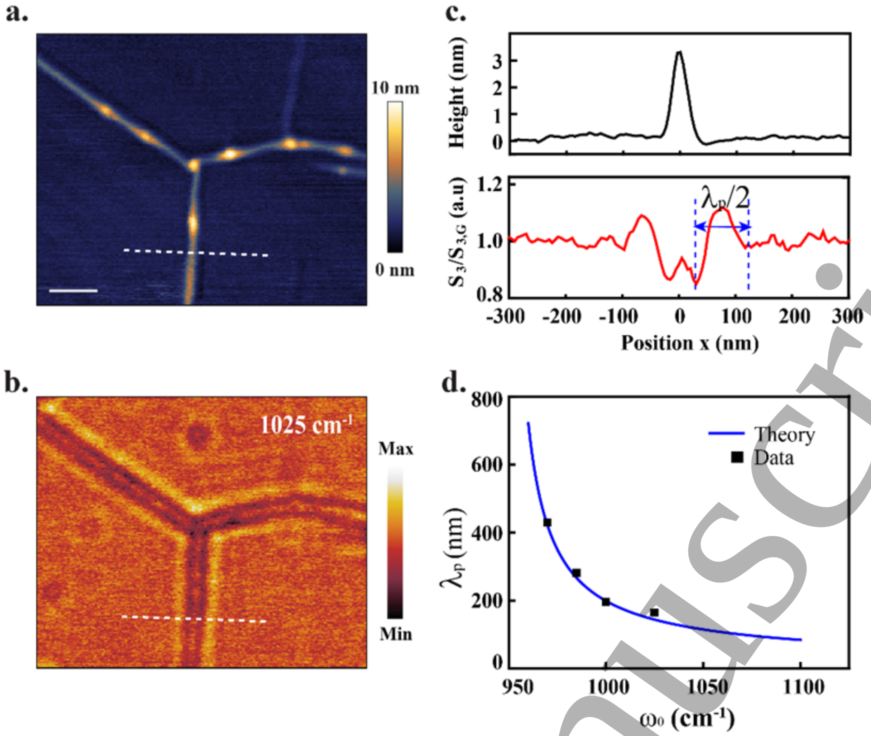

Figure. 3 The dispersion of graphene plasmons on SiC substrate. (a) Topography image of a 1*1 um area in **Fig. 1b**. (b) The infrared near field imaging of (a) at the frequency of 1025 cm^{-1}. (c) Topography height (upper) and normalized near field amplitude (lower) of line profiles taken along the white dash lines in (a) and (b). (d) Relationship of graphene plasmons wavelength and incident frequency. The blue curve and black square represent the theoretical result and experimental data, respectively. The scale bar is 200 nm.

It is reported[36] that the epitaxial graphene on SiC is doped because of the interaction with the substrate. Obviously, due to the compressive force[24], the wrinkle is separated with the SiC substrate at the narrow region, which means a weaker interaction with the substrate and resulted in a low doping from SiC to graphene wrinkles. In this paper, we suppose that the Fermi energy at the wrinkle changes simultaneously with the increase height of wrinkle for simply. Thus we assume that the Fermi level at the wrinkle is decreasing with a Gaussian shape profile $E_F(x) = E_F(\infty) * (1 - \delta e^{-x^2/w^2})$, where $E_F(\infty) = 0.18\ eV$ is the Fermi energy far away from the wrinkle corresponding to a carrier density of $n = 2.4 * 10^{12}\ cm^{-2}$ which agrees with the holes carrier concentration measured in the epitaxial monolayer graphene on SiC $(11\bar{2}0)$ substrate,[37, 38] w is the width of the wrinkle determined by the height profile of wrinkle and δ is the variation of Fermi energy relative to that of flat graphene. By adjusting the variation $\delta = 0.8$, we fit the experiment data with the simulation result (more simulation is shown in Supporting Information) as the red line in **Figure 4(b)**, which shows a great agreement with the experiment. It is clear that the plasmons reflection of wrinkle is cause of the variation of Fermi energy instead of the geometry corrugation. For achieving a more physical understanding and analysis of the graphene plasmons reflection by wrinkle, we calculate the spatial distribution of $|E_Z|$ around the wrinkle with and without a variation of conductivity in **Figure 4(c)** and **(d)**. In the case of a constant conductivity of wrinkle, the spatial electric field $|E_Z|$ indicate that the plasmons propagate through the wrinkle directly with a negligible reflection. Otherwise, in the case of a relative decreased conductivity ($\delta = 0.8$), $|E_Z|$ shows interference fringes on the left of wrinkle, which also suggests a strong reflection by the wrinkle.[29]

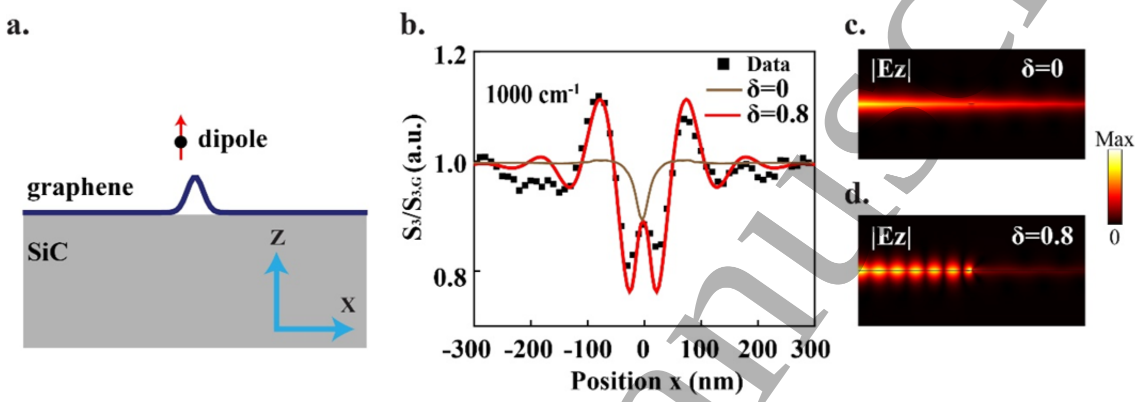

Figure. 4 The simulation of graphene plasmons reflected by the wrinkle (a) The schematic of simulation model. (b) Comparison of experimental data (black square) and simulation results (solid line) with different variation of Fermi energy. (c), (d) The spatial distribution of $|E_z|$ corresponding to different variation of Fermi energy. The scale is 50 nm.

According to the d.c. conductivity[27] $\sigma_{dc} \approx (2e^2/h)(E_F/E_\tau)$, the decreased Fermi energy results to a reduced local d.c. conductivity of graphene. Therefore, the region around the wrinkle can be regarded as a heterojunction with a localized variation in electronic property. Besides, it also suggests that the localized electronic property related with Fermi energy has a relationship with the height of wrinkle, as the different plasmons reflection shown in **Figure 1** and **Figure S2**. Simulated with different variation of Fermi energy (i.e. d.c. conductivity) (see in **Figure S5**), it shows that a rapidly and sharply varied d.c. conductivity causes a strong plasmons reflection and a slowly and slightly varied d.c. conductivity causes a weak plasmons reflection. The wrinkle with a height below 1 nm has a slowly varied electronic property, which is important to the fabrication of a homogenous epitaxial graphene electronic device.

3. Conclusion

Above all, utilizing the scattering near-field scanning optical microscopy, we study the influence of wrinkle to the graphene plasmons. The near field imaging of graphene plasmons around the graphene wrinkles shows a novel reflection factor. Combined with the numerical simulation results, we point out that the geometry corrugation has a negligible plasmons reflection when the height of wrinkle $h \ll \lambda_p$. It is important to point out that the wrinkle separated from the substrate has a lower doping level, which means a nonlinear localized electronic property at the wrinkle. The wrinkle with a height below 1 nm has a slowly varying electronic property, which leads to a negligible reflection of graphene plasmons. While a taller wrinkle causes obvious varying of electronic property, which gives rise to stronger plasmons reflection. This work offers a new sight to know the electronic properties of graphene wrinkle and reveal that wrinkles can be seen as a nanoscale tunable damper for further plasmonics and optoelectronic applications.

4. Method

4.1 Graphene preparation

The monolayer graphene was epitaxial growth on the nonpolar silicon carbon $(11\bar{2}0)$ by a thermal decomposition method,[39] where the graphene raised up and separated from the substrate then the wrinkle formed due to the different thermal expansion coefficients of graphene and SiC substrate during the cooling process.

4.2 Experiment measurements

Raman measurements: The Raman spectra are measured with a Raman spectrometer with excitation laser of 532 nm. The spot size focused on the sample is about 1 um with a 100x objective, and the power of the laser is about 1 mW. The grating spectrometer is 1800/mm, make sure to achieve a resolution about 0.2 cm^{-1} of Raman spectra.

Near field s-SNOM measurements: The near field infrared nano-image experiments are conducted by the scattering-type scanning near field optical microscopy (s-SNOM) from Neaspec GmbH. Based on an atomic force microscopy (AFM) which works with a tapping mode at frequency about 300 kHz and amplitude about 30 nm. The incident infrared light is obtained by the quantum cascade lasers, with a power of 5 mW.

4.3 Calculation of plasmons dispersion

The theoretical relation of graphene plasmons on SiC substrate which is determined[27] by $\lambda_p(\omega) = \frac{\pi\sigma(\omega)}{i\omega\varepsilon_0\kappa(\omega)}$, where ε_0 is the permittivity of vacuum, $\sigma(\omega)$ is the optical conductivity of graphene, $\kappa(\omega) = [1 + \varepsilon_{sub}(\omega)]/2$ and $\varepsilon_{sub}(\omega)$ is the dielectric function of SiC substrate. For a limit of long wavelength and low frequency, the optical conductivity can be written as Drude model[21] $\sigma(\omega) = i\frac{e^2}{\pi\hbar^2}\frac{E_F}{\omega+i\tau^{-1}}$, where τ is the relaxation time and E_F is Fermi energy.

4.4 Numerical simulation

The near field simulation of graphene wrinkle by a point dipole model and the spatial distribution of $|E_z|$ around the wrinkle are obtained by the finite element method using the commercial software Comsol. The mesh in our model is fine enough to achieve a good convergence result. The permittivity of SiC is taken from the literature.[40]

Supporting Information

Supporting Information Available: Raman Mapping image of graphene sample, more details experiment and simulation results of graphene plasmons reflected by the wrinkles.

Acknowledgements

We thank Alexey Nikitin for original simulation modeling ideas and discussions.

References

[1] Ritchie R H 1957 *Physical Review D* **106** 874
[2] Barnes W L, Dereux A and Ebbesen T W 2003 *Nature* **424** 824
[3] Gramotnev D K and Bozhevolnyi S I 2010 *Nature Photonics* **4** 83
[4] Chen W, Hu H, Jiang W, Xu Y, Zhang S and Xu H 2018 *Chinese Physics B* **27** 107403
[5] Qurban M, Tahira R, Ge G-Q and Ikram M 2019 *Chinese Physics B* **28** 030304
[6] Lu H, Fan Y-C, Dai S-Q, Mao D, Xiao F-J, Li P and Zhao J-L 2018 *Chinese Physics B* **27** 117302
[7] Chuan-Pu Liu X-L Z, Jia-Sen Zhang, Jun Xu, Yamin Leprince-Wang, Da-Peng Yu 2016 *Chinese Physics Letters* **33** 87303
[8] Cheng Zi-Qiang S H-Q, Yu Ping, Liu Zhi-Min 2018 *Acta Physica Sinica* **67** 197302
[9] Geim A K and Novoselov K S 2010 *Nanoscience and Technology: A Collection of Reviews from Nature Journals* (World Scientific) pp. 11-19
[10] Bolotin K I, Sikes K, Jiang Z, Klima M, Fudenberg G, Hone J, Kim P and Stormer H 2008 *Solid State Communications* **146** 351
[11] Ju L, Geng B, Horng J, Girit C, Martin M, Hao Z, Bechtel H A, Liang X, Zettl A and Shen Y R 2011 *Nature nanotechnology* **6** 630
[12] Fang Z, Thongrattanasiri S, Schlather A, Liu Z, Ma L, Wang Y, Ajayan P M, Nordlander P, Halas N J and García de Abajo F J 2013 *ACS nano* **7** 2388
[13] Fang Z, Wang Y, Liu Z, Schlather A, Ajayan P M, Koppens F H, Nordlander P and Halas N J 2012 *ACS nano* **6** 10222
[14] Chen J, Badioli M, Alonsogonzalez P, Thongrattanasiri S, Huth F, Osmond J, Spasenovic M, Centeno A, Pesquera A and Godignon P 2012 *Nature* **487** 77
[15] Fei Z, Rodin A S, Andreev G O, Bao W, Mcleod A S, Wagner M, Zhang L M, Zhao Z, Thiemens M H and Dominguez G 2012 *Nature* **487** 82
[16] Abajo D and Garcia F J 2014 *ACS Photonics* **1** 135
[17] Hupalo M, Conrad E and Tringides M 2009 *Physical Review B* **80** 041401
[18] De Heer W A, Berger C, Ruan M, Sprinkle M, Li X, Hu Y, Zhang B, Hankinson J and Conrad E 2011 *Proceedings of the National Academy of Sciences* **108** 16900
[19] Novoselov K S, Geim A K, Morozov S V, Jiang D, Zhang Y, Dubonos S V, Grigorieva I V and Firsov A A 2004 *science* **306** 666
[20] Lu J, Loh K P, Huang H, Chen W and Wee A T 2009 *Physical Review B* **80** 113410

[21] Chen J, Nesterov M L, Nikitin A Y, Thongrattanasiri S, Alonsogonzalez P, Slipchenko T M, Speck F, Ostler M, Seyller T and Crassee I 2013 *Nano Letters* **13** 6210
[22] Fang Z, Liu Z, Wang Y, Ajayan P M, Nordlander P and Halas N J 2012 *Nano Letters* **12** 3808
[23] Fang Z, Wang Y, Schlather A E, Liu Z, Ajayan P M, García de Abajo F J, Nordlander P, Zhu X and Halas N J 2013 *Nano Letters* **14** 299
[24] Deng S and Berry V 2016 *Materials Today* **19** 197
[25] Bao W, Miao F, Chen Z, Zhang H, Jang W, Dames C and Lau C N 2009 *Nature nanotechnology* **4** 562
[26] Zhu W, Low T, Perebeinos V, Bol A A, Zhu Y, Yan H, Tersoff J and Avouris P 2012 *Nano Letters* **12** 3431
[27] Fei Z, Rodin A S, Gannett W, Dai S, Regan W, Wagner M, Liu M, Mcleod A S, Dominguez G and Thiemens M H 2013 *Nature Nanotechnology* **8** 821
[28] Garcia-Pomar J L, Nikitin A Y and Martin-Moreno L 2013 *ACS nano* **7** 4988
[29] Slipchenko T M, Nesterov M L, Hillenbrand R, Nikitin A Y and Martín-Moreno L 2017 *ACS Photonics* **4** 3081
[30] Ocelic N, Huber A J and Hillenbrand R 2006 *Applied Physics Letters* **89** 101124
[31] Yang R, Huang Q, Chen X, Zhang G and Gao H-J 2010 *Journal of Applied Physics* **107** 034305
[32] Ferrari A C and Basko D M 2013 *Nature Nanotechnology* **8** 235
[33] Malard L, Pimenta M, Dresselhaus G and Dresselhaus M 2009 *Physics Reports* **473** 51
[34] Graf D, Molitor F, Ensslin K, Stampfer C, Jungen A, Hierold C and Wirtz L 2007 *Nano Letters* **7** 238
[35] Ferrari A C 2007 *Solid State Communications* **143** 47
[36] Sidorov A N, Gaskill K, Buongiorno Nardelli M, Tedesco J L, Myers-Ward R L, Eddy Jr C R, Jayasekera T, Kim K W, Jayasingha R and Sherehiy A 2012 *Journal of Applied Physics* **111** 113706
[37] Camara N, Jouault B, Caboni A, Tiberj A, Godignon P and Camassel J 2011 *Nanoscience and Nanotechnology Letters* **3** 49
[38] Jabakhanji B, Camara N, Caboni A, Consejo C, Jouault B, Godignon P and Camassel J *Materials Science Forum*, p. 235-241
[39] Jia Y, Guo L, Lu W, Guo Y, Lin J, Zhu K, Chen L, Huang Q, Huang J and Li Z 2013 *Science China-physics Mechanics & Astronomy* **56** 2386
[40] Mutschke H, Andersen A C, Clement D, Henning T and Peiter G 1999 *Astronomy and Astrophysics* **345** 187